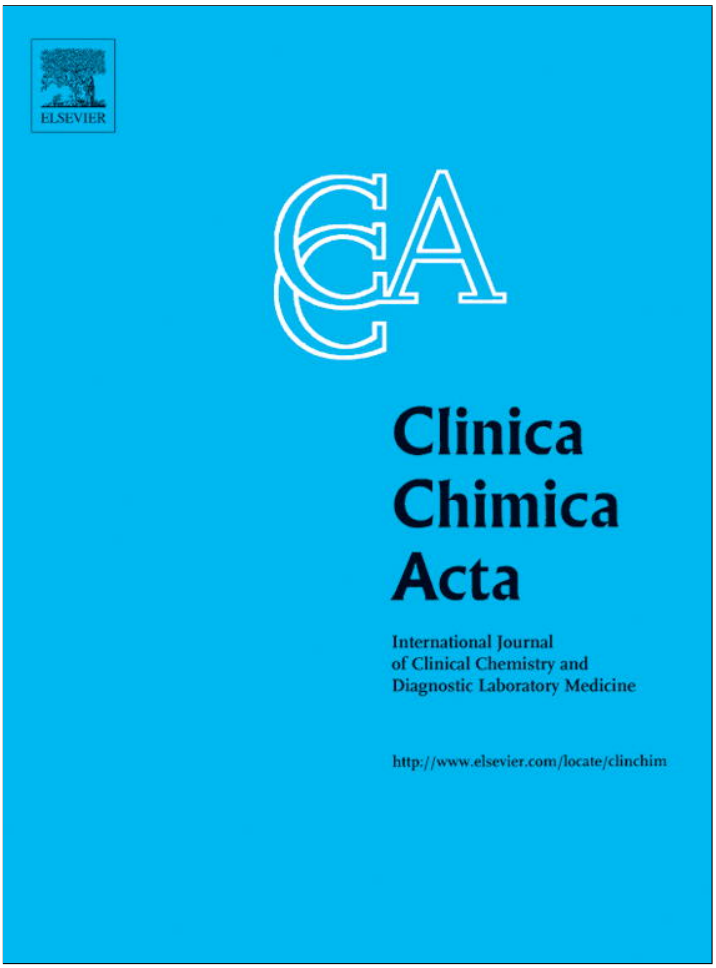

Clinica Chimica Acta 446 (2015) 86–92

Contents lists available at ScienceDirect

Clinica Chimica Acta

journal homepage: www.elsevier.com/locate/clinchim

Improving arylsulfatase activity determination in dried blood spots: Screening and diagnostic approaches for Maroteaux–Lamy syndrome (MPS VI)

Paula G. Franco [a,b], María J. Pérez [a,b], Claudio Aranda [c], Ana Adamo [a,b], Lucas Silvestroff [a,b,*]

[a] Departamento de Química Biológica Patológica, Facultad de Farmacia y Bioquímica, Universidad de Buenos Aires, Buenos Aires, Argentina
[b] Instituto de Química y Fisicoquímica Biológicas "Prof. Alejandro E. Paladini" (IQUIFIB, UBA-CONICET), Buenos Aires, Argentina
[c] Hospital General de Agudos Carlos G. Durand, Ciudad Autónoma de Buenos Aires, Argentina

ARTICLE INFO

Article history:
Received 2 October 2014
Received in revised form 27 March 2015
Accepted 8 April 2015
Available online 18 April 2015

Keywords:
Arylsulfatase B
Newborn screening
Quenching
Methylumbelliferone
Enzyme activity
Fluorescence

ABSTRACT

Background: Mucopolysaccharidosis type VI can be screened by measuring the lysosomal arylsulfatase B (ARSB) residual enzyme activity in dried blood spots (DBS) using synthetic substrates. However, we have found experimental obstacles when determining ARSB activity with the fluorescent method due to the significant quenching effect rendered by DBS components.
Methods: We adapted the methods originally described by Chamoles et al. [1] and Civallero et al. [2] and put forward 2 distinct approaches for ARSB activity quantification from DBS samples by measuring the 4-methylumbelliferone (β-MU) fluorescence generated from the ARSB 4-methylumbelliferone sulfate (β-MUS) substrate.
Results: We demonstrate the high throughput feasibility of a novel approach for measuring ARSB activities by incorporating tailor-made calibration curves according to each patient's DBS sample quenching properties. The second method is used to calculate ARSB activities by measuring the fluorescence and absorbance parameters in each reaction sample with a single DBS-free calibration curve.
Conclusions: The quantitative correlation between the DBS sample absorbance and its quenching effect can be used to calculate predictive ARSB activities and would serve as an affordable first tier screening test. The method described herein demonstrates the critical importance of adapting the β-MU calibration curves to each patient's unique DBS sample matrix and its positive impact on the accuracy and reliability of ARSB activity measurements.

1. Introduction

The fluorescence-based method for detecting lysosomal storage disorder (LSD) has been adapted to newborn screening (NBS), where different β-MU-derived substrates are used to quantitate decreased lysosomal enzyme activities in DBS samples from newborns [1,3]. One such example is that of the B isoform of arylsulfatase (ARSB, EC 3.1.6.12) or *N*-acetylgalactosamine-4-sulfatase, a lysosomal enzyme that is affected in patients with the Mucopolysaccharidosis type VI (MPS VI) rare disease, or Maroteaux–Lamy syndrome (OMIM# 253200, Valayannopoulos et al., 2010) [4]. Treatment for MPS VI is now available and includes enzyme replacement therapies and cell therapies [5,6]. The fact that early treatment improves MPS VI patient's outcome reinforces the importance of its detection before clinical onset [7,8].

The measurement of ARSB enzyme is performed using β-methylumbelliferone sulfate (β-MUS) as a substrate, which renders β-MU after its specific enzymatic cleavage. Although the β-MU molecule is highly fluorescent, its detection is seriously hampered when it is found in a matrix rich in blood components, such as that derived from DBS. The negative effect of blood compounds on the detection of β-MU fluorescence is termed *quenching* and was previously described for other enzymatic reactions involving β-MU fluorescence detection [9].

To quantitate β-MU generation after the enzymatic reaction, the sample fluorescence is interpolated in β-MU calibration curves. However, β-MU calibrators are usually prepared in an aqueous matrix lacking blood components. Therefore, the enzyme activity (EA) calculated by interpolating sample fluorescence values in a blood-free calibration curve provides data that underestimate the real EA. A common strategy to rid the quenching effect when measuring EA in blood-derived samples is to precipitate proteins after the reaction takes place [10]. However, in our experience, precipitation is rarely achieved completely, and the β-MUS substrate appears to be particularly sensitive to

Abbreviations: ARSB, arylsulfatase B isoform; AU, arbitrary units; DBS, dried blood spot; EA, enzyme activity; LSD, lysosomal storage disorder; MPS VI, mucopolysaccharidosis type VI; NBS, newborn screening; β-MU, 4-methylumbelliferone; β-MUS, 4-methylumbelliferone sulfate.

* Corresponding author at: Junín 956 (C1113AAD), Ciudad Autónoma de Buenos Aires, Argentina. Tel./fax: +1 5411 4964 8287.
E-mail address: lsilver81@yahoo.com.ar (L. Silvestroff).

http://dx.doi.org/10.1016/j.cca.2015.04.011
0009-8981/

precipitating agents, resulting in high non-enzymatic hydrolysis values (unpublished results).

In the present work, we propose a revised method for the fluorometric determination of lysosomal EA in dried blood spots where the undesired quenching effects of blood components on β-MU fluorescence are overcome. Furthermore, the protocol we put forward provides a novel strategy to measure the ARSB enzyme activity in an accurate manner in DBS so as to complement urine glycosaminoglycan level quantitations, molecular analysis, and other clinical findings during MPS VI diagnosis [11].

2. Materials and methods

2.1. Materials

β-Methylumbelliferone, sodium salt, 4-methylumbelliferyl sulfate potassium salt, bovine serum albumin, and βmethylumbelliferyl *N*-acetyl-β-glucosaminide were from Sigma Aldrich. Sodium acetate was from Mallinckrodt, lead acetate from Baker, glycine was from Biopak, heparin was from Nortia, ethylenediamine from Sintorgan, and anhydrous citric acid from Anedra.

2.2. Samples

All biological samples were from human origin. Methodological optimization of enzyme activity determination was performed with DBS samples corresponding to three healthy adults (one male and two females of 32, 35, and 43 years) with no prior history of lysosomal-related pathology. Individuals with more than 6 h of fasting donated blood voluntarily and signed a written informed consent. After extraction, blood was immediately spotted onto Schleicher and Schuell 903 (S&S 903) filter paper (Guthrie cards). An aliquot of whole blood was dispensed in a conical tube, incubated at 37 °C for 1 h, and centrifuged for 5 min at 6,700×*g* at room temperature for serum isolation. A second aliquot was mixed with 10 μl of 5,000 IU/L heparin for plasma separation. Whole heparinized blood, serum, and plasma were then spotted onto Guthrie cards. All the samples were left to dry overnight at room temperature and then stored at −20 °C.

For the *screening* approach protocol, anonymous DBS samples from neonates were obtained from Hospital General de Agudos *Carlos G. Durand* (Ciudad Autónoma de Buenos Aires, Argentina). The DBS were transported in a sealed envelope at room temperature and then stored at 4 °C. All the DBS used in this study were punched with a final diameter of 1/8″ (3.2 mm).

2.3. ARSB enzymatic reaction

Reactions were all set up in 1.5 ml microtubes. For initial experiments, the DBS punches were pooled in water for 45 min at room temperature (30 μl of distilled water per 3.2 mm Ø DBS) to obtain a homogeneous eluate. The basic reaction protocol was modified from Civallero et al. [2]. Briefly, the reaction tubes were prepared by adding the following components: 10 μl of a sodium acetate (525 mM)–lead acetate (45 mmol/l) buffered solution (pH 5), 75 μl of a β-MUS (10 mM) aqueous solution, and 30 μl of the DBS pooled eluate. The mixture was then completed with distilled water to 150 μl. The reaction was incubated at 37 °C for 20 h, after which it was stopped by adding 450 μl of a glycine (85 mM)-NaOH-buffered solution (pH 10.5). After stopping the reaction, the samples were centrifuged at room temperature for 2 min at 11,300×*g*. Fluorescence was measured in 200 μl aliquots of each tube dispensed in 96-well white plates.

The calibration curves were prepared in different matrices (described in the text and shown in Supplementary Data Table 1) by adding different volumes of a 0.3 mM β-MU standard solution. Reaction samples and calibration tubes contained the same final volume, buffer concentration, and pH and were processed in parallel.

All enzyme activity values are expressed as nmol/ml/h, where the units represent the β-MU nanomoles formed in 1 ml of whole blood per hour, considering that a 3.2 mm diameter DBS contains 3.6 μl of whole blood as previously reported by Civallero et al. [2]. For serum and plasma spotted samples, we considered sample volume/spot as equal to that of a DBS. The Bradford assay was performed by adding 200 μl of the Bradford solution to 2 μl of the stopped reaction samples. For measuring the DBS sample raw absorbance, a 200 μl aliquot of the stopped enzyme reaction was directly placed in 96-well plates and read in a spectrophotometer at 405 nm.

2.4. Total hexosaminidase enzymatic reaction

The protocol was performed as described by Civallero et al. [2]. In addition, we included reaction tubes with β-MU internal standard, as described in Supplementary Table 1, in order to measure the enzyme activity using the same *SuSi* method as used for ARSB, and as described in Section 3.

2.5. Fluorescence

Fluorescence was measured using a Perkin Elmer LS 55 Fluorescence Spectrometer. Excitation and emission wavelengths were set at 365 nm and 450 nm, respectively, except for the initial emission spectrum profile shown in Fig. 1A, where excitation wavelength was fixed at 365 nm while the emission wavelength was scanned from 200 to 700 nm. The photomultiplier voltage, mirror slits, and detection time were adjusted to maximize the reading values.

2.6. Statistical analysis

All graphs and statistical analysis were performed with the GraphPad Prism Software. Statistical data for individual experiments are indicated in figures and table legends.

3. Results

3.1. Blood component effect on β-MU fluorescence

The negative effects of blood components on the β-MU fluorescence detection were confirmed by analyzing the fluorescence emission spectrum of 5 nmol of β-MU at a fixed excitation wavelength (365 nm) and in the presence or absence of a DBS belonging to a healthy adult (Fig. 1A). The detection of β-MU fluorescence was hampered by blood components at all emission wavelengths compared to the DBS-free condition. The β-MU fluorescence peak was observed at 451 nm and showed a 95% decrease when DBS components were present (Fig. 1A). At these wavelengths, we did not detect auto-fluorescence belonging to blood components or the buffer.

We analyzed the β-MU fluorescence in two calibration curves; one was built in buffer and was termed *W* due to its *water*-like transparent appearance, the other was prepared with a DBS eluate and was termed *Q* because of its quenching matrix (Supplementary Data Table 1, Fig. 1B, Supplementary Data Table 3). The DBS-derived quenching effect on the fluorescence was constant (≈95%) at all the assayed β-MU concentrations of the calibration curve (Fig. 1C).

The ARSB activity was measured by interpolating the β-MU fluorescence generated by ARSB-specific hydrolysis of β-MUS, in both *W* and *Q* calibration curves for comparison. Since the detection of β-MU in the DBS reaction mixture is unavoidably subjected to the blood component-derived quenching, the use of a *Q* curve would be a better approach, as the β-MU would be exposed to the same degree of quenching.

The fact that DBS eluates from 194 healthy newborns showed *Q* quenching effects on fluorescence ranging between 74% and 93% (data

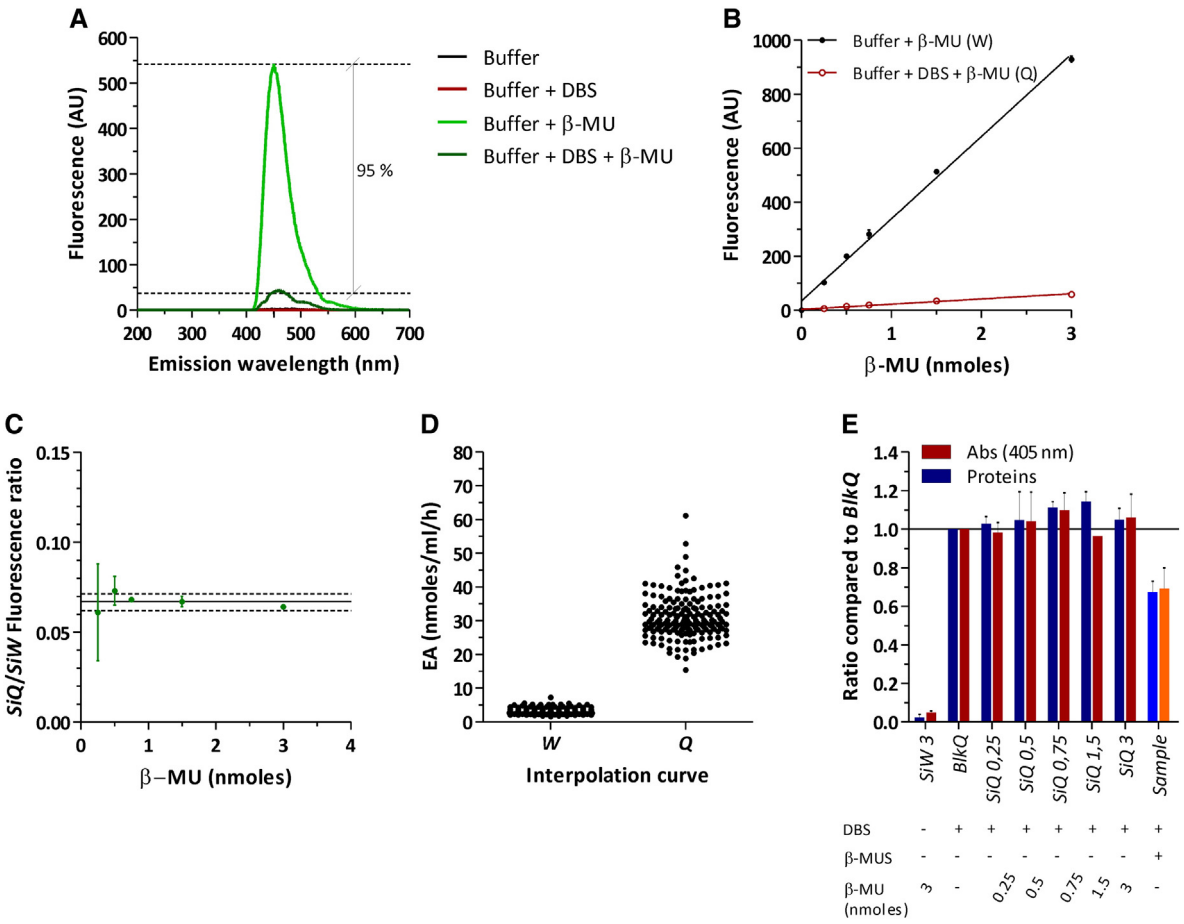

Fig. 1. (A) Variation of β-MU emission spectra (5 nmol/200 μl) at a fixed 365 nm excitation wavelength. The horizontal dotted lines represent the β-MU maximum fluorescence values at an excitation wavelength of 451 nm for the "Buffer + β-MU" and the "Buffer + DBS + β-MU" conditions. (B) Fluorescence of β-MU calibration curves in the absence (*W*) or presence (*Q*) of a DBS. (C) Fluorescence ratios of β-MU at different concentrations in the *Q*-quenched calibration (+ DBS) curve compared to a *W* (DBS-free) calibration curve. The solid horizontal line indicates the mean (0.067) and the dotted lines indicate the SD (0.0046). (D) Enzyme activity of ARSB in DBS of healthy term newborns according to the calibration curves used to interpolate β-MU fluorescence. (E) Protein concentration and absorbance (405 nm) of DBS components from a healthy adult in the reaction supernatant after 20 h of incubation. All data in each series are expressed as a ratio compared to the 0 nmol β-MU of the calibration curve (Blank, *BlkQ*). Si: β-MU internal standard; W, indicates the reaction matrix is free of blood components. Data belong to duplicates of a single experiment. Error bars represent the SD. The DBS used for A-C and E were from a healthy adult.

not shown) excluded the possibility of using a single generic *Q* curve for all samples.

Thus, we built individual *Q* curves for each sample by using β-MU calibrators in the presence of DBS components. We also prepared the sample reaction tube containing the β-MUS substrate together with the DBS to determine the ARSB activity. The EA was calculated by interpolating the fluorescence value from the reaction tube in its own *Q*-quenched calibration curve (EA_Q). This EA was compared to that obtained from interpolating the sample fluorescence in an unquenched DBS-free calibration curve (EA_W). EA_Q was on average 10-fold higher than EA_W curve (Fig. 1D). At this point, we concluded that adding each patient's DBS to the calibrators allowed us to build a tailor-made *Q* curve for each sample and avoid underestimating the real EA.

3.2. The Q and q quenching effects

After the 20 h incubation required for the reaction completion, however, we noticed that the reaction tubes containing the DBS components and the β-MUS substrate (DBS + β-MUS) had a residue lying at the bottom of the tubes. Moreover, the remaining supernatant had a paler color (orange tone) than the more intense red-colored tubes belonging to the *Q*-quenched calibration curve (DBS + β-MU).

We separated the supernatants after centrifugation and measured the total amount of soluble proteins by the Bradford method and the absorbance at 405 nm, according to the blood spectrophotometric absorbance spectra (Fig. 1E). The absorbance at 405 nm was used as a direct method to quantify sample color. We found both measurements decreased more than 30% in the orange-colored reaction sample (DBS + β-MUS) compared to the red-colored *Q* calibration curve (DBS + β-MU) (Fig. 1E, Table 1). The 30% decrease in protein concentration and supernatant absorbance in the *Sample* reaction is a direct consequence of a fraction of blood components being dragged along with the lead sulfate precipitate that is formed *in situ* as the enzymatic reaction progresses. The removal of blood components with quenching capacity unmasks the β-MU real fluorescence (Supplementary Data Fig. 1A, B).

On this ground, if protein concentration and absorbance differences affected fluorescence detection, we would be interpolating the reaction tube fluorescence in a red-colored *Q* curve, leading to the overestimation of β-MU production. We *a priori* indexed the orange-colored sample reaction matrix *q* in opposition to the high red-coloured *Q* curves previously described.

3.3. The SuSiq method

Since our aim was to maintain the sample reaction matrix most alike to the calibration curve matrix, we found the current quenched *Q* curve

Table 1
Components used to prepare the DBS-free calibration curve (*W*), the DBS-containing calibration quenched curve (*Q*), and the sample enzymatic reaction mixture (DBS + β-MUS). β-MU, 4-methylumbelliferone standard; β-MUS, substrate 4-methylumbelliferyl sulfate; DBS, dried blood spot; *Q*, high quenching matrix; *q*, low quenching matrix; *W*, no quenching.

Tube	β-MUS	β-MU	DBS	Incubation	Insoluble residue	Color	Abs. 405 nm (%)[a]	Proteins (%)[a]	Quenching
W curve	–	Yes	–	Yes	–	Transparent	–	–	*W*
Q curve	–	Yes	Yes	Yes	–	Red	100	100	*Q*
Sample reaction	Yes	–	Yes	Yes	Present	Orange	30–50	30–50	*q*

[a] Total soluble protein and absorbance at 405 nm measurements were performed on supernatants obtained after the 20-h incubation period.

method was unsuitable for interpolating the *q*-quenched reaction sample fluorescence values.

The *q*-quenched matrix seemed to develop when DBS and substrate were incubated together in the reaction tube. We evaluated the incorporation of the β-MU standard into the reaction tube and used the term *Si* (internal standard) to indicate if the β-MU was present as such. In this case, the DBS components, the β-MUS substrate, and the β-MU standard were mixed together during incubation to generate *q*-quenched matrices. This reaction tube with β-MU as an internal standard was run in parallel with reaction tubes lacking the added standard. A formula was built to describe the components that provide fluorescent β-MU nanomoles in the reaction tube containing the internal β-MU standard (*SuSi* tube) (1), where the β-MU fluorescence was generated from the internal standard and the β-MUS substrate cleavage.

$$\text{Total } \beta\text{-MU} = \beta\text{-MU(generated from substrate)} + \beta\text{-MU(internal standard)} \quad (1)$$

The matched reaction tube without standard only contained β-MU generated by β-MUS cleavage (*Su* tube). Since both tubes contained the DBS components and the β-MUS substrate, they had a precipitate at the end of the incubation period, and the supernatants were both *q*-quenched (Supplementary Data Fig. 1A, B). We added the *q* suffix to identify the *q*-quenched matrix; *Suq* and *SuSiq* (Table 2). The theoretical *Siq* fluorescence can be calculated by subtracting *Suq* fluorescence from *SuSiq*;

$$Siq = SuSiq - Suq \quad (2)$$

With the *Siq* data obtained by adding variable and known amounts of the β-MU standard in the *SuSiq* tubes, we built a *q* calibration curve in which to interpolate the fluorescence obtained from the *Suq* sample tubes (Fig. 2A).

As expected, the calculated *q* curve passes through zero when there are no β-MU nmol present. Furthermore, the total protein content and the absorbance (405 nm) parameters were maintained constant at increasing *Si* nmol, indicating the *q* quenching was comparable in the different *SuSiq* tubes (Fig. 2B, Table 2).

For practical reasons, we selected a single β-MU standard concentration to build the *Q* and *q*-quenched calibration curves (Fig. 1B). We set the β-MU internal standard concentration at 2.5 mM in the *SiQ* and *SuSiq* tubes (0.5 nmol in the 200 μl aliquot used to measure fluorescence) for the remaining experiments, and linear regression was calculated by forcing the curves through zero. We verified β-MU can be added to the *SuSiq* reaction mixture up to a 15 mM final concentration without disturbing the ARSB enzymatic activity (Fig. 2A, See Supplementary Data Table 4).

The protein concentration and the 405 nm absorbance parameters were measured in the different *SiQ*, *Suq*, and *SuSiq* tubes to demonstrate DBS components differentially impact β-MU fluorescence according to the *q* or *Q* quenching effects (Fig. 2B, C and Supplementary Data Fig. 2).

We performed additional studies to confirm optimal substrate concentration and incubation time was preserved under this modified methodology (See Supplementary Data Fig. 3).

Table 2
Components used to prepare the *Suq* and *SuSiq* reaction mixtures. β-MU, 4-methylumbelliferone standard; β-MUS, 4-methylumbelliferyl sulfate; DBS, dried blood spot.

Tube	β-MUS	β-MU	DBS	Incubation	Insoluble residue	Color	Quenching
Suq	Yes	–	Yes	Yes	Present	Orange	*q*
SuSiq	Yes	Yes	Yes	Yes	Present	Orange	*q*

[a] Total soluble protein and absorbance at 405 nm measurements were performed on supernatants obtained after the 20-h incubation period.

3.4. ARSB activity in different blood-derived samples

The consequence of interpolating the β-MU fluorescence generated from 192 newborn DBS samples (*Suq* = *reaction tube*) in a *q*-quenched calibration curve (*Siq*) allowed us to obtain EA values closer to what we consider are real values.

The EA obtained from using the *SuSiq* method was termed EA_q and rendered values that were 40% lower than those obtained when using a *Q* curve (EA_Q), but more than 4-fold higher than when using the *W* curve (EA_W) (Fig. 1D, see Supplementary Data Table 5).

The *SuSiq* method was applied on DBS from newborns and adults to compare the EA_q values (Fig. 3A). We observed that the mean values among populations of healthy newborns, premature newborns, and healthy adults were not significantly different (Fig. 3A, B).

We analyzed the ARSB enzyme activity in serum and plasma samples obtained from 3 healthy adults and compared their values according to the serum and plasma calibration curves, respectively. We also used DBS in the presence or absence of heparin to rule out possible interferences. We observed that heparin did not affect the ARSB activity in the DBS samples. Plasma and serum displayed similar ARSB EA_q and did not vary according to the calibration curve used (water matrix, or in the presence of serum/plasma with or without substrate). Nevertheless, we noticed serum and plasma had a substantial reduction in EA compared to that of DBS (Fig. 3B).

Total hexosaminidase (HexT) enzyme activity was determined in newborn DBS samples as a control assay of lysosomal enzyme function by reproducing a similar approach as for ARSB. Since there was no precipitate formed in HexT reactions, the quenching properties were equal in all the tubes containing DBS eluates. However, we considered the use of the Internal Standard method (*SuSi*) was the most appropriate in terms of its independence from variations between the quenched matrix of samples and their own quenched calibration curves (Fig. 3C). The HexT activity was increased 10-fold when interpolating the sample fluorescence values in the appropriate *Q*-quenched calibration curve (1304 ± 582 nmol/ml/h) than when using a single *W* curve (140.4 ± 83 nmol/ml/h) (Fig. 3D).

3.5. An approach to newborn screening: the Fq method

The above-mentioned *SuSiq* method is suggested for diagnostic purposes. However, for screening high numbers of samples, sufficient DBS samples for each patient are required. Besides, the number of tubes analyzed would double if *Suq* and *SuSiq* reaction tubes were prepared for each patient. We continued searching for a method that

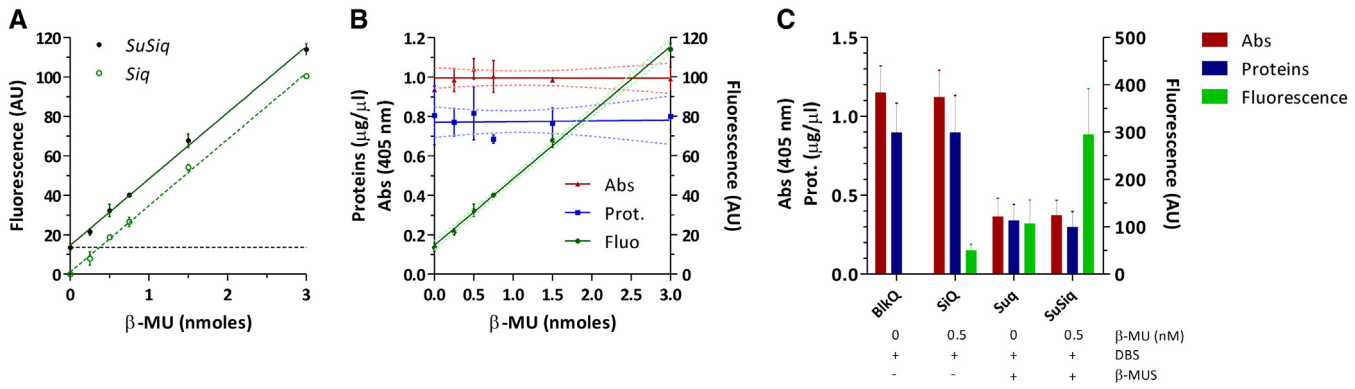

Fig. 2. (A) The horizontal line indicates fluorescence in the *Suq* reaction. (B) Absorbance (405 nm), protein concentration (μg/ml), and the *SuSiq* calibration curve are shown as a function of the nanomoles of β-MU added to the *SuSiq* samples. The β-MU nanomoles on the *x*-axis of *A* and *B* represent the nanomoles present in a 200 μl aliquot of the samples used to read fluorescence. (C) Correlation between protein concentration, absorbance, and fluorescence of *BlkQ*, *SiQ*, *Suq*, and *SuSiq* reactions when using DBS from three healthy adults. β-MU final concentration was 2.5 mM for all tubes containing *Si*. Error bars in all graphs represent the SD.

could better adapt to massive DBS analysis with a view to a possible application in an expanded NBS Program.

By establishing the relationship between the sample absorbance (405 nm) and the *q* quenching effect on β-MU fluorescence, we might be able to use an accessible and unsophisticated parameter to correct the sample's quenched fluorescence. The theoretical unquenched value calculated could then be interpolated in a single *W* curve. If we compare the fluorescence for a given β-MU concentration in the quenched reaction tube ($Fluo_q$) and in an unquenched water matrix ($Fluo_W$), we can determine the following relationship:

$$Fluo_W = Fluo_q . Fq \quad (3)$$

where Fq is a quenching correction factor proportional to the *q* quenching effect. Therefore, we evaluated if sample absorbance measurement was a reliable parameter to estimate the degree of *q*

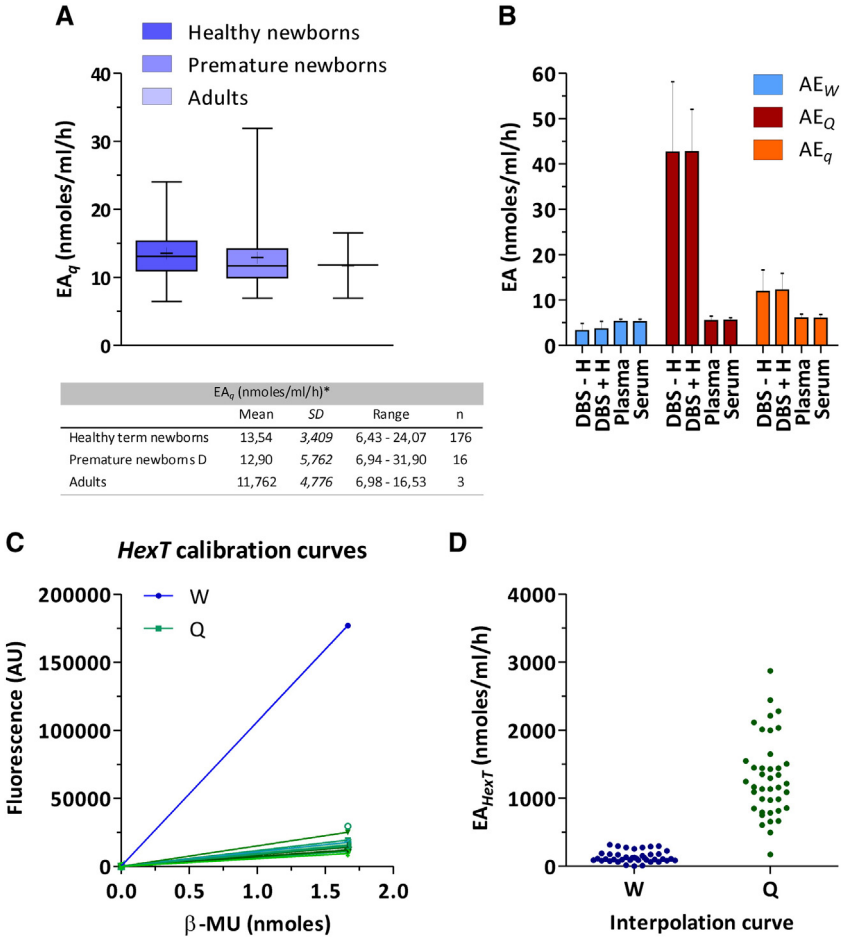

EA$_q$ (nmoles/ml/h)*	Mean	SD	Range	n
Healthy term newborns	13,54	3,409	6,43 - 24,07	176
Premature newborns D	12,90	5,762	6,94 - 31,90	16
Adults	11,762	4,776	6,98 - 16,53	3

Fig. 3. (A) The ARSB EA_q was measured in different populations of newborns and adults. All EA_q were obtained by interpolating the *Suq* values in each *q* calibration curve. The boxes represent the interquartile range and the whiskers represent the 1st–99th percentile. The cross (+) within the boxes indicates the population mean value. (B) Comparison of the ARSB EA_q values obtained from different samples of adults, and when the *Suq* fluorescence values are interpolated in the different calibration curves; *W*, *Q*, and *q*. Error bars represent the SD. H, heparin; DBS, dried blood spot. (C) β-MU calibration curves for HexT EA calculation. (D) HexT EA data from 40 neonates by interpolating fluorescence in calibration curves shown in C.

quenching. The *Siq* fluorescence was calculated as previously described in healthy newborn DBS samples and represents the β-MU fluorescence in a *q*-quenched matrix ($Fluo_q$). The fluorescence of an equal β-MU concentration was measured in water and was considered the maximal fluorescence in a *W* unquenched matrix ($Fluo_W$). For each sample, Fq was calculated as the $Fluo_W/Fluo_q$ ratio and the *Suq* absorbance (405 nm) was measured as well. When graphing Fq as a function of *Suq* sample absorbance (405 nm), we found that the R^2 for the linear regression ($R^2 = 0.84$) was slightly higher than that for the one-phase exponential regression ($R^2 = 0.80$) (Fig. 4A). However, we chose the non-linear regression analysis since it better adjusted to patients with low absorbance values. The non-linear regression curve equation was given by

$$Fq = Fq0.\ e^{(k.\ Abs)} \quad (4)$$

The *k* value is a constant, and *Fq0* is the *y*-intercept that equals 1 when the $Fluo_W$ and $Fluo_q$ are hypothetically equal. Eqs. (3) and (4) were re-arranged so that the raw absorbance (Abs) and fluorescence ($Fluo_q$) measurements of a single *Suq* reaction tube could be used to calculate a theoretical unquenched β-MU fluorescence ($Fluo_W$):

$$Fluo_W = Fluo_q.\ e^{(k.\ Abs)} \quad (5)$$

$Fluo_W$ values for each sample were then interpolated in a single generic β-MU *W* curve to obtain nanomoles formed during reaction. The EA calculated by this method was termed EA_{FqW}. Setting a cutoff value for EA_{FqW} in the 5th percentile (8.452 nmol/ml/h) might allow us to identify possible ARSB deficiency candidates for further follow-up in a screening program.

Comparison of EA from samples obtained by the *SuSiq* (EA_q) and *Fq* (EA_{FqW}) methods (Fig. 4B) showed a significant correlation with Pearson's test (see Supplementary Data Table 6), and the EA_q/EA_{FqW} ratio was in average 1,004 (Fig. 4C).

4. Discussion

In this work, we were able to address and overcome methodological obstacles involved in the ARSB EA measurement, and ensured that the EA_q obtained with the internal standard method (*SuSiq*) were closer to the sample's values than when a unique calibration curve is used for all samples. Secondly, we provide a strategy to include ARSB measurement in an expanded NBS program where many samples must be analyzed with a robust and unsophisticated technique.

We based our protocol on that reported by Civallero et al. [2] and assumed the reaction was specific for the ARSB isoform since adding $AgNO_3$ (0.3 mM final concentration), an ARSA isoform inhibitor, did not alter the DBS-derived EA (data not shown) [12,13]. Insofar, the precipitate formation seems to be specific to the 4-methylumbelliferyl sulfate potassium salt, where insoluble lead sulfate salts are generated from the substrate hydrolysis and the reaction buffer lead ions.

Although two simultaneous reaction tubes are required for measuring the EA_q, the *SuSiq* method is more accessible than previously reported ARSB enzyme immunocapture assays [14] and could be easier to set up in every-day laboratory work in developing countries.

Moreover, the *SuSiq* method becomes a valuable tool to rid EA values of systematic errors during diagnosis that could lead to false interpretations. If the quenching effect is not considered, samples from patients with low hemoglobin blood concentrations might result in higher fluorescence readings (lower quenching) and consequently favor falsely high enzyme activities.

Clinically diagnosed MPS VI patient samples will be required to determine ARSB EA distribution and compared to that of healthy individuals. However, the *SuSiq* method should contribute and/or complement other diagnostic methods for this disease in the future [15,16], or even be used for prenatal diagnosis [17].

The Fq method is proposed for its use in an NBS program since it requires a single *Suq* reaction compared to the *SuSiq* method. Besides, the EA_{FqW} obtained with the Fq method incorporates an inherent quenching correction since the sample's absorbance measurement must be considered in the EA calculation process. Similar to the *SuSiq* method, incorporating the absorbance parameter in the EA calculation avoids false results when individual DBS have a lower quenching effect than average.

We do stress the fact that the Fq method requires an initial setup in each laboratory, where the mathematical correlation existing between the *q*-quenched *Suq* sample absorbance and the Fq fluorescence correction factor must be established. Similar to Shigeto et al. (2011) [10], we describe an exponential correlation between β-MU fluorescence and blood hemoglobin absorbance.

As a whole, we propose the Fq method for screening ARSB EA in a wide population screening program, and the *SuSiq* method for further diagnostic purposes [18]. Our approach can even be extended to ARSB EA analyses in DBS from high risk populations [19]. Most importantly, the incorporation of an internal standard can be extended to other EA measurements with β-MU-derived substrates for the detection of LSD, where blood components play such important quenching effects when using DBS samples.

Supplementary data to this article can be found online at http://dx.doi.org/10.1016/j.cca.2015.04.011.

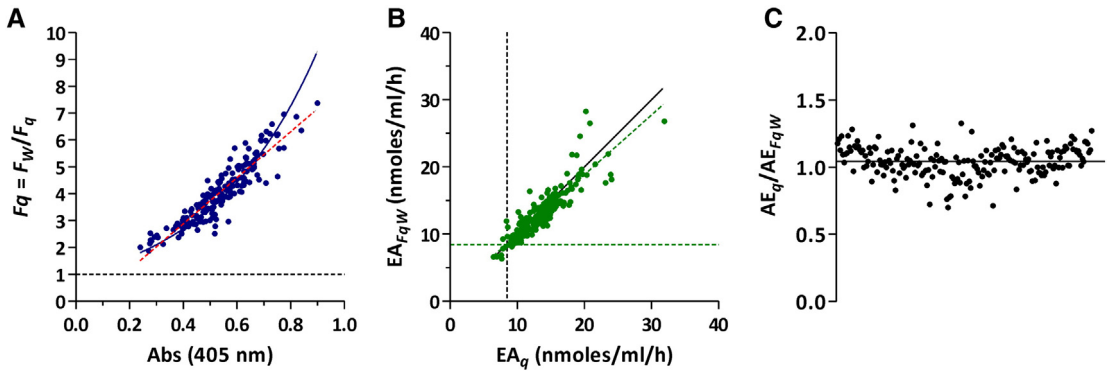

Fig. 4. (A) The Fq value is plotted as a function of the *SuSiq* sample absorbance. The horizontal dotted line indicates the lowest possible Fq value. The *linear regression* line is indicated in red and the *non-linear regression* curve is indicated in blue. (B) Correlation between the EA obtained by the *SuSiq* and Fq methods (EA_q and EA_{FqW}, respectively). The black dotted lines represent the lowest 5th percentile of the EA obtained with the *SuSiq* method (vertical dotted line) or the Fq method (horizontal dotted line). The oblique solid lines represent the linear regression expected if there was a perfect correlation (black) and the real regression line that correlated the calculated EA values (green). (C) The EA_q/EA_{FqW} ratio is represented for 194 newborns, where the overall ratio mean was 1.004, an SD of 0.1119, and a range between 0.7011 and 0.9744.

Acknowledgements

This work was funded by the Argentine Agencia Nacional de Promoción Científica y Tecnológica (Préstamo BID PICT 2011-2040), CONICET (PIP 711), and the Universidad de Buenos Aires (UBACyT # 20020120100132BA). The funders had no decision on the study design, result interpretation, or manuscript preparation.

References

[1] Chamoles N, Blanco M, Gaggioli D. Diagnosis of α-L-iduronidase deficiency in dried blood spots on filter paper: the possibility of newborn diagnosis. Clin Chem 2001; 47:780–1.
[2] Civallero G, Michelin K, de Mari J, Viapiana M, Burin M, Coelho J, et al. Twelve different enzyme assays on dried-blood filter paper samples for detection of patients with selected inherited lysosomal storage diseases. Clin Chim Acta 2006;372:98–102.
[3] Chamoles N, Blanco M, Gaggioli D. Fabry disease: enzymatic diagnosis in dried blood spots on filter paper. Clin Chim Acta 2001;308:195–6.
[4] Valayannopoulos V, Nicely H, Harmatz P, Turbeville S. Mucopolysaccharidosis VI. Orphanet J Rare Dis 2010;5:5.
[5] Giugliani R, Harmatz P, Wraith JE. Management guidelines for mucopolysaccharidosis VI. Pediatrics 2007;120(2):405–18.
[6] Harmatz P, Garcia P, Guffon N, Randolph L, Shediac R, Braunlin E, et al. Galsulfase (Naglazyme®) therapy in infants with mucopolysaccharidosis VI. J Inherit Metab Dis 2014;37:277–87.
[7] Jester S1, Larsson J, Eklund EA, Papadopoulou D, Månsson JE, Békássy AN, et al. Haploidentical stem cell transplantation in two children with mucopolysaccharidosis VI: clinical and biochemical outcome. Orphanet J Rare Dis 2013;8:134.
[8] Kampmann C, Lampe C, Whybra-Trümpler C, Wiethoff CM, Mengel E, Arash L, et al. Mucopolysaccharidosis VI: cardiac involvement and the impact of enzyme replacement therapy. J Inherit Metab Dis 2014;37:269–76.
[9] Oemardien L, Boer A, Ruijter G, van der Ploeg A, de Klerk J, Reuser A, et al. Hemoglobin precipitation greatly improves 4-methylumbelliferone-based diagnostic assays for lysosomal storage diseases in dried blood spots. Mol Genet Metab 2011;102:44–8.
[10] Shigeto S, Katafuchi T, Okada Y, Nakamura K, Endo F, Okuyama T, et al. Improved assay for differential diagnosis between Pompe disease and acid α-glucosidase pseudodeficiency on dried blood spots. Mol Genet Metab 2011;103:12–7.
[11] Mendelsohn N, Wood T, Olson R, Temme R, Hale S, Zhang H, et al. Spondyloepiphyseal dysplasias and bilateral legg-calvé-perthes disease: diagnostic considerations for mucopolysaccharidoses. JIMD Rep 2013;11:125–32.
[12] Rip J, Gordon B. A simple spectrophotometric enzyme assay with absolute specificity for arylsulfatase A. Clin Biochem 1998;31:29–31.
[13] Martino S, Consiglio A, Cavalieri C, Tiribuzi R, Costanzi E, Severini G, et al. Expression and purification of a human, soluble arylsulfatase A for metachromatic leukodystrophy enzyme replacement therapy. J Biotechnol 2005;117:243–51.
[14] Hein L, Meikle P, Dean C, Bockmann M, Auclair D, Hopwood J, et al. Development of an assay for the detection of mucopolysaccharidosis type VI patients using dried blood-spots. Clin Chim Acta 2005;353:67–74.
[15] Garrido E, Chabás A, Coll M, Blanco M, Domínguez C, Grinberg D, et al. Identification of the molecular defects in Spanish and Argentinian mucopolysaccharidosis VI (Maroteaux–Lamy syndrome) patients, including 9 novel mutations. Mol Genet Metab 2007;92:122–30.
[16] Lachman R, Burton B, Clarke L, Hoffinger S, Ikegawa S, Jin D, et al. Mucopolysaccharidosis IVA (Morquio A syndrome) and VI (Maroteaux–Lamy syndrome): under-recognized and challenging to diagnose. Skeletal Radiol 2014;43:359–69.
[17] Burin M, Ribeiro E, Mari J, Schwartz I, Martins M, Giugliani R. Prenatal diagnosis of mucopolysaccharidosis VI by enzyme assay in a dried spot of fetal blood: a pioneering case report. Prenat Diagn 2010;30:89–90.
[18] Wood T, Bodamer O, Burin M, D'Almeida V, Fietz M, Giugliani R, et al. Expert recommendations for the laboratory diagnosis of MPS VI. Mol Genet Metab 2012; 106:73–82.
[19] Castilhos CD, Mezzalira J, Goldim MP, Daitx VV, Garcia Cda S, Andrade CV, et al. Determination of the lysosomal hydrolase activity in blood collected on filter paper, an alternative to screen high risk populations. Gene 2014;536(2):344–7.